

Parameter uncertainties for imperfect surrogate models in the low-noise regime

Thomas D. Swinburne*

Aix-Marseille Université, CNRS, CINaM UMR 7325, Campus de Luminy, 13288 Marseille, France

Danny Perez†

Theoretical Division T-1, Los Alamos National Laboratory, Los Alamos, USA

(Dated: December 1, 2024)

Bayesian regression determines model parameters by minimizing the expected loss, an upper bound to the true generalization error. However, the loss ignores misspecification, where models are imperfect. Parameter uncertainties from Bayesian regression are thus significantly underestimated and vanish in the large data limit. This is particularly problematic when building models of low-noise, or near-deterministic, calculations, as the main source of uncertainty is neglected. We analyze the generalization error of misspecified, near-deterministic surrogate models, a regime of broad relevance in science and engineering. We show posterior distributions must cover every training point to avoid a divergent generalization error and design an *ansatz* that respects this constraint, which for linear models incurs minimal overhead. This is demonstrated on model problems before application to thousand dimensional datasets in atomistic machine learning. Our efficient misspecification-aware scheme gives accurate prediction and bounding of test errors where existing schemes fail, allowing this important source of uncertainty to be incorporated in computational workflows.

Surrogate models are widely used across science and engineering to efficiently approximate the action of computationally intensive simulation engines [1–7]. Domain expertise is leveraged to design optimal features and model architecture before parameters are inferred from training data generated by the engines. In a broad range of applications, the inference problem shares three key characteristics:

- a) Simulation engines are near *deterministic*: outputs have vanishing aleatoric uncertainty, e.g. the atomic energy $V(\mathbf{X})$ is deterministic to atomic positions \mathbf{X} .
- b) Surrogate models are *misspecified*: no single choice of the P parameters can match all N observations, meaning parameters are intrinsically uncertain.
- c) Surrogate models are *underparametrized*: large quantities of training data are available, such that standard epistemic uncertainty estimates from Bayesian inference vanish, typically corresponding to the regime $P/N \ll 1$.

Misspecification affects both finite capacity models and deep learning approaches with finite training resources [8, 9]. A misspecification-aware learning scheme should minimize the cross entropy between predicted and observed data distributions, known as the *generalization error*, or under certain technical definitions, the population risk (see [10, 11]). However, the generalization error is typically not tractable for learning, both due to numerical instabilities and the lack of theoretical bounds for convergence. Bayesian learning schemes instead minimize an upper bound, the *expected loss* (log likelihood), which ignores misspecification but admits a robust learning scheme. Epistemic uncertainties are thus severely underestimated, vanishing in the underparametrized limit, with broad implications for surrogate model selection, uncertainty quantification

and error propagation, as noted by multiple groups [8, 9, 12–15].

In this paper, we analyze the generalization error of deterministic, misspecified and under-parametrized surrogate models, i.e. those typically used to approximate simulation engines in science and engineering. As posterior distributions strictly become unbounded in the deterministic limit, this is only taken as a theoretical device to derive conditions that any posterior must obey to avoid a divergent generalization error. We then design an *ansatz* that respects this condition and admits a robust learning scheme at finite N , with standard treatment of epistemic (N -dependent) errors, reducing to a constrained loss minimization problem for large N/P . Our final misspecification-aware parameter posterior has finite uncertainty even as $N/P \rightarrow \infty$ with a provably lower generalization error than the Gibbs posterior of Bayesian inference.

Our main contributions are:

- a) We define *pointwise optimal parameter sets* (POPS) for each training point, within which model predictions are exact. Parameter distributions must have mass in every POPS to avoid a divergent generalization error.
- b) We use the ensemble of loss minimizers from each POPS to design two *ansatz* posteriors, a reweighted $\mathcal{O}(N)$ ensemble and a bounding $\mathcal{O}(P)$ hypercube, both of which respect POPS occupancy and give a finite generalization error, lower than the Gibbs posterior from inference.
- c) For linear models, our *ansatz* can be efficiently evaluated via rank-one updates to a leverage-weighted loss minimizer. This gives an efficient scheme to incorporate misspecification into linear regression with minimal computational overhead.
- d) We test the approach on synthetic datasets, show-

ing how our scheme provides robust bounds on test errors. This performance is maintained under application to thousand-dimensional datasets from atomic machine learning, untreatable with existing methods.

Related work

Germain and coworkers [16] established an important connection between Bayesian inference and probability approximately correct (PAC-Bayes) analysis for regression problems with unbounded losses, which bounds true expectations by empirical likelihood expectations through concentration inequalities. This provides a robust learning scheme without test-train splitting, and gives a rationalization for Bayesian inference as a form of regularization. In particular, minimizing the PAC-Bayes bound for the expected loss gives the familiar relation between posterior, prior and likelihood from Bayesian inference.

In recent years, multiple groups have used the PAC-Bayes framework to derive tighter bounds for the generalization error than that provided by the expected loss [8, 9, 11, 12, 14, 16]. However, these efforts focus on probabilistic regression settings, often with neural network models far from the underparametrized limit, meaning aleatoric, epistemic and misspecification errors must be considered jointly.

Masegosa [12] derived second order PAC-Bayes bounds for the generalization error minimized through a variational or ensemble *ansatz*. Morningstar *et al.* [11] developed estimators to assess disagreement between the generalization error and expected loss, deriving specialized PAC bounds for theoretical guarantees. Lahou *et al.* [8] considered misspecification of neural networks, jointly training a minimum loss surrogate and an independent predictor of misspecification error. Lofti *et al.* [14] considered misspecification in the context of deep model selection, deriving conditional likelihoods better aligned with the generalization error.

As various definitions for the distinction between epistemic and misspecification uncertainties exist [13], we define misspecification as non-aleatoric uncertainties which survive in the underparametrized limit, where the minimizer of PAC-Bayes bounds for the expected loss, which coincides with the posterior from Bayesian inference, predict vanishing parameter uncertainties. This definition is made more precise in section . Our epistemic uncertainties thus coincide with standard estimates from loss minimization.

BAYESIAN SURROGATE MODELS

Deterministic simulation engines

A simulation engine $\mathcal{E} : \mathcal{X} \rightarrow \mathcal{Y}$ takes input $\mathbf{X} \in \mathcal{X}$ and returns $\mathbf{Y} \in \mathcal{Y}$. We consider the regime where the aleatoric uncertainty of \mathcal{E} is weak and can be described as a Gaussian distribution with mean $\langle \mathbf{Y} | \mathbf{X} \rangle \equiv \mathcal{E}(\mathbf{X})$ and covariance $\langle \mathbf{Y} \mathbf{Y}^\top | \mathbf{X} \rangle - \mathcal{E}(\mathbf{X}) \mathcal{E}^\top(\mathbf{X}) \equiv \Sigma_{\mathcal{Y}}(\mathbf{X})$, where $\|\Sigma_{\mathcal{Y}}(\mathbf{X})\| = \mathcal{O}(\epsilon^{2Y})$, and ϵ is assumed small. The true conditional output distribution thus reads

$$\rho_{\mathcal{E}}(\mathbf{Y} | \mathbf{X}) = \mathcal{N}(\mathbf{Y} | \mathcal{E}(\mathbf{X}), \Sigma_{\mathcal{Y}}(\mathbf{X})). \quad (1)$$

We assume homoskedatiscity $\Sigma_{\mathcal{Y}}(\mathbf{X}) = \Sigma_{\mathcal{Y}}$ of this weak aleatoric error to investigate the deterministic, underparametrised limit $\epsilon \rightarrow 0$, $N/P \rightarrow \infty$ for $\epsilon = \mathcal{O}(\sqrt{P/N})$. With weights $\sum_{i=1}^N w_i = 1$, the training configurations $\mathcal{D}_N = \{\mathbf{Y}_i, \mathbf{X}_i\}_{i=1}^N$ form an input distribution in \mathbf{X} of

$$\rho_N(\mathbf{X}) \equiv \sum_i w_i \delta(\mathbf{X} - \mathbf{X}_i), \quad \rho_{\mathcal{D}}(\mathbf{X}) \equiv \lim_{N \rightarrow \infty} \rho_N(\mathbf{X}). \quad (2)$$

Learning requires that we can bound expectations over independent identically distributed (i.i.d.) samples $\mathbf{X}, \mathbf{Y} \in \mathcal{D}$

$$\langle f(\mathbf{Y}, \mathbf{X}) \rangle_{\mathcal{D}} \equiv \int_{\mathcal{D}} f(\mathbf{Y}, \mathbf{X}) \rho_{\mathcal{E}}(\mathbf{Y} | \mathbf{X}) \rho_{\mathcal{D}}(\mathbf{X}) d\mathbf{X} d\mathbf{Y}. \quad (3)$$

For timeseries or other signal data the i.i.d. property is only satisfied for decorrelated segments $\mathbf{X} = \{\mathbf{x}_t\}_{t=1}^T$, meaning $\Sigma_{\mathcal{Y}}(\mathbf{X})$ captures signal correlations as in generalized least squares regression.

Deterministic surrogate models

A surrogate model $\mathcal{M} : \mathcal{X} \rightarrow \mathcal{Y}$ for \mathcal{E} is defined by P parameters $\Theta \in \mathcal{P}$. Under a parameter distribution $\pi(\Theta)$, the predicted distribution has the same form as (1), reading

$$\rho_{\mathcal{M}}(\mathbf{Y} | \mathbf{X}, \Theta) = \mathcal{N}(\mathbf{Y} | \mathcal{M}(\mathbf{X}, \Theta), \Sigma_{\mathcal{Y}}), \quad (4)$$

$$\rho_{\mathcal{M}}(\mathbf{Y} | \mathbf{X}) = \int_{\mathcal{P}} \rho_{\mathcal{M}}(\mathbf{Y} | \mathbf{X}, \Theta) \pi(\Theta) d\Theta. \quad (5)$$

Unlike typical Bayesian schemes, we do not treat the covariance term $\Sigma_{\mathcal{Y}}$ as fitting parameter but as an intrinsic property of \mathcal{E} . This has implications for model selection criteria, discussed in the supplementary material (SM) [17].

The generalization error and expected loss

The generalization error $\mathcal{G}[\pi]$ is simply the cross entropy of the predicted distribution $\rho_{\mathcal{M}}(\mathbf{Y} | \mathbf{X}) \rho_N(\mathbf{X})$ to

the observed distribution $\rho(\mathbf{Y}|\mathbf{X})\rho_N(\mathbf{X})$; omitting the constant term $\mathcal{G}_{\mathcal{E}} \equiv \langle \ln |\rho_{\mathcal{E}}(\mathbf{Y}|\mathbf{X})| \rangle_{\mathcal{D}}$ we have

$$\mathcal{G}[\pi] = - \left\langle \ln \left| \int_{\mathcal{P}} \rho_{\mathcal{M}}(\mathbf{Y}|\mathbf{X}, \Theta) \pi(\Theta) d\Theta \right| \right\rangle_{\mathcal{D}}. \quad (6)$$

In principle any learning scheme should aim to minimize the non-convex functional $\mathcal{G}[\pi]$, but in practice learning schemes target a convex upper bound, the *expected loss* $\mathcal{L}[\pi] \geq \mathcal{G}[\pi]$, often known as the negative log likelihood. Using the Jensen inequality $-\langle \ln x \rangle \leq -\ln \langle x \rangle$ gives

$$\mathcal{G}[\pi] \leq \mathcal{L}[\pi] = - \int_{\mathcal{P}} \langle \ln |\rho_{\mathcal{M}}(\mathbf{Y}|\mathbf{X}, \Theta)| \rangle_{\mathcal{D}} \pi(\Theta) d\Theta. \quad (7)$$

$\mathcal{L}[\pi]$ is clearly minimized by a delta function $\delta(\Theta - \Theta_{\mathcal{L}}^*)$, where $\Theta_{\mathcal{L}}^* \in \arg \min_{\Theta \in \mathcal{P}} \langle -\ln |\rho_{\mathcal{M}}(\mathbf{Y}|\mathbf{X}, \Theta)| \rangle_{\mathcal{D}}$, i.e. vanishing parameter uncertainty. The next section shows how this emerges from the inference posterior at finite N/P .

PAC-Bayes estimation and connection to inference

PAC-Bayes analysis [10] provides concentration inequalities [18] that bound expectations over \mathcal{D} by empirical expectations over \mathcal{D}_N with some probability. Whilst originally designed for classification problems, the approach has been extended to regression settings with unbounded losses [16]. As discussed in the SM [17], The expected loss $\mathcal{L}[\pi]$ admits the PAC-Bayes upper bound, holding with probability $1 - \xi$, of

$$\mathcal{L}[\pi] \leq \int_{\mathcal{P}} \hat{L}_N(\Theta) + \frac{1}{N} \ln \left| \frac{\pi}{\pi_0} \right| d\pi(\Theta) - \frac{\ln |\xi|}{N} + C_0, \quad (8)$$

where $\hat{L}_N(\Theta) = -\langle \ln |\rho_{\mathcal{M}}(\mathbf{Y}|\mathbf{X}, \Theta)| \rangle_N$ is the empirical loss over $\rho_N(\mathbf{X})$, $\pi_0(\Theta)$ is some *prior* and C_0 is a constant [17]. The minimizer of the upper bound (21) is the posterior from Bayesian inference [16]

$$\pi_{\mathcal{L},N}(\Theta) = \pi_0(\Theta) \exp(\lambda - N\hat{L}_N(\Theta)). \quad (9)$$

As $N/P \rightarrow \infty$ the posterior is strongly peaked around a loss minimizer $\Theta_{\mathcal{L}}^* \in \arg \min_{\Theta \in \mathcal{P}} L(\Theta)$. Defining Σ_0^{-1} as the curvature of $-\ln \pi_0(\Theta)$ around $\Theta_{\mathcal{L}}^*$, we use Laplace's method [17] as $N/P \rightarrow \infty$ to write

$$\pi_{\mathcal{L}}(\Theta) = \mathcal{N}(\Theta | \Theta_{\mathcal{L}}^*, [\Sigma_0 + N\mathcal{I}_{\mathcal{L}}^*]^{-1}), \quad (10)$$

where $\mathcal{I}_{\mathcal{L}}^* \equiv \lim_{N/P \rightarrow \infty} \nabla_{\Theta} \nabla_{\Theta}^{\top} \hat{L}_N(\Theta_{\mathcal{L}}^*)$ is the Fisher information matrix. If $\mathcal{I}_{\mathcal{L}}^*$ is full rank the prior has vanishing influence and the expected loss is minimized by the sharp distribution $\pi_{\mathcal{L}}(\Theta) \rightarrow \delta(\Theta - \Theta_{\mathcal{L}}^*)$, giving vanishing parameter uncertainty. Otherwise, the inference prior may still have finite width but, by construction, these will not have influence on model predictions. In either case, it is clear that generalization error of the loss minimizing distribution diverges as $1/\epsilon^2$:

$$\lim_{N/P \rightarrow \infty} \mathcal{G}[\pi_{\mathcal{L}}] = \frac{1}{2} \text{Tr}(\Sigma_{\mathcal{L}}^* \Sigma_{\mathcal{Y}}^{-1}) = \mathcal{O}(1/\epsilon^2). \quad (11)$$

$\Sigma_{\mathcal{L}}^* = \langle [\mathcal{E}(\mathbf{X}) - \mathcal{M}(\mathbf{X}, \Theta_{\mathcal{L}}^*)][\mathcal{E}(\mathbf{X}) - \mathcal{M}(\mathbf{X}, \Theta_{\mathcal{L}}^*)]^{\top} \rangle$ is the error covariance around $\Theta_{\mathcal{L}}^*$ and we use $\text{Tr}(\Sigma_{\mathcal{Y}}) = \mathcal{O}(\epsilon^2)$. Under misspecification it is thus clear that minimizing this upper bound is sub-optimal [12] as the generalization error diverges as $1/\epsilon^2$. In the next section we analyze the generalization error as $\epsilon \rightarrow 0$ to derive a condition for any $\pi(\Theta)$ that ensures a finite generalization error.

ANALYSIS OF THE GENERALIZATION ERROR IN THE NEAR-DETERMINISTIC LIMIT

We consider the generalization error (6) in the near-deterministic limit, $\mathcal{G}_0[\pi] \equiv \lim_{\epsilon \rightarrow 0} \mathcal{G}[\pi]$. The integral over \mathbf{Y} in (6) concentrates at $\mathbf{Y} = \mathcal{E}(\mathbf{X})$; using $\langle \dots \rangle_{\mathcal{X}} \equiv \int \dots \rho_{\mathcal{D}}(\mathbf{X}) d\mathbf{X}$ yields, using Laplace's method [17]

$$\begin{aligned} \mathcal{G}_0[\pi] &= -\langle \ln |\rho_{\mathcal{M}}(\mathcal{E}(\mathbf{X})|\mathbf{X})| \rangle_{\mathcal{X}} \\ &= -\left\langle \ln \left| \int_{\mathcal{P}} \rho_{\mathcal{M}}(\mathcal{E}(\mathbf{X})|\mathbf{X}, \Theta) \pi(\Theta) d\Theta \right| \right\rangle_{\mathcal{X}}. \end{aligned} \quad (12)$$

Whilst $\mathbf{Y} = \mathcal{E}(\mathbf{X})$ is a unique maximum, to ensure $\min_{\mathbf{X} \in \mathcal{X}} \rho_{\mathcal{M}}(\mathcal{E}(\mathbf{X})|\mathbf{X}) > 0$ and thus avoid divergence in $\mathcal{G}_0[\pi]$ as $\epsilon \rightarrow 0$ we require $\pi(\Theta)$ has mass in every *pointwise optimal parameter set* (POPS)

$$\mathcal{P}_{\mathcal{M}}(\mathbf{X}) \equiv \{\Theta | \mathcal{M}(\mathbf{X}, \Theta) = \mathcal{E}(\mathbf{X})\}. \quad (13)$$

Any model with a constant term will ensure $\mathcal{P}_{\mathcal{M}}(\mathbf{X}) \neq \emptyset$, but under misspecification it clear that $\cap_{\mathbf{X} \in \mathcal{X}} \mathcal{P}_{\mathcal{M}}(\mathbf{X}) = \emptyset$.

To express the final generalization error, we introduce a pointwise mass function

$$m_{\mathcal{E}}(\Theta, \mathbf{X}) \equiv \int_{\mathcal{P}} \delta(\Theta - \Theta') \rho_{\mathcal{M}}(\mathcal{E}(\mathbf{X})|\mathbf{X}, \Theta') d\Theta',$$

which gives our first main result, a generalization error for deterministic surrogate models of

$$\mathcal{G}_0[\pi] \equiv -\left\langle \ln \int_{\mathcal{P}} m_{\mathcal{E}}(\Theta, \mathbf{X}) \pi(\Theta) d\Theta \right\rangle_{\mathcal{X}}. \quad (14)$$

To avoid $1/\epsilon^2$ divergence in $\mathcal{G}_0[\pi]$ a valid $\pi(\Theta)$ must satisfy the 'POPS covering' constraint as $\epsilon \rightarrow 0$ of

$$\min_{\mathbf{X} \in \mathcal{X}} \max_{\Theta \in \mathcal{P}_{\mathcal{M}}(\mathbf{X})} \pi(\Theta) > \lim_{\epsilon \rightarrow 0} \exp(-c/\epsilon^2), \quad (15)$$

for any $c > 0$. Equation (15) is our second main result, a demonstration that any candidate minimizer of the generalization error must have probability mass in every POPS $\mathcal{P}_{\mathcal{M}}(\mathbf{X})$, whilst the minimizing distribution concentrates on regions where multiple POPS intersect. As shown above, the minimum loss solution $\pi_{\mathcal{L}}(\Theta)$ does not satisfy this requirement and thus $\mathcal{G}[\pi_{\mathcal{L}}] = \mathcal{O}(1/\epsilon^2)$. Importantly, when (15) is satisfied, the predictive distribution $\rho_{\mathcal{M}}(\mathbf{Y}, \mathbf{X})$ covers every training data point,

i.e. model predictions will envelope observations as $N/P \rightarrow \infty$. We now investigate two candidate distributions which satisfy (15), an $\mathcal{O}(N)$ ensemble *ansatz* and $\mathcal{O}(P)$ hypercube *ansatz*, finding approximate variational minima that allow for efficient deployment on high-dimensional datasets.

POPS-constrained ensemble and hypercube *ansatz*

The covering constraint (15) requires $\pi(\Theta)$ to have mass in the POPS of each training point. This condition must be satisfied whilst concentrating mass in as small a region in \mathcal{P} as possible to minimize \mathcal{G}_0 . To achieve this, we first select a set of pointwise fits $\Theta_{\mathbf{X}}^* \in \mathcal{T}_E^*$ that are each POPS-constrained loss minimizers

$$\Theta_{\mathbf{X}}^* \in \mathcal{T}_E^*, \quad \Theta_{\mathbf{X}}^* \equiv \arg \min_{\Theta_{\mathbf{X}} \in \mathcal{P}_{\mathcal{M}}(\mathbf{X})} L(\Theta_{\mathbf{X}}). \quad (16)$$

These pointwise fits will be closely clustered around the minimum loss solution $\Theta_{\mathcal{L}}^*$, as measured by the Fisher metric $\mathcal{I}_{\mathcal{L}}^*$. In the supplementary materials [17] we explore a weighted ensemble *ansatz*

$$\pi_E^*(\Theta) = \langle w(\mathbf{X}) \delta(\Theta - \Theta_{\mathbf{X}}^*) \rangle, \quad (17)$$

where $w(\mathbf{X}) > 0$. In particular, we show \mathcal{T}_E^* naturally emerges when choosing pointwise fits $\Theta_{\mathbf{X}} \in \mathcal{P}_{\mathcal{M}}(\mathbf{X})$ to minimize the *ansatz* expected loss $\mathcal{L}[\pi_E] = \langle w(\mathbf{X}) L(\Theta_{\mathbf{X}}) \rangle$.

The ensemble *ansatz* produces highly informative max/min bounds for any test point, providing an envelope for worst case errors, as we show in figure 1. However, even when employing an optimal reweighting $w^*(\mathbf{X})$ (see [17]), the ensemble *ansatz* systematically underestimates moments of the test error distribution, as shown in figure 2. In addition, both resampling and storage are $\mathcal{O}(N)$, which can become problematic for the $N/P \rightarrow \infty$ limit of interest.

For practical applications, the parameter distribution should ideally require at most $\mathcal{O}(P^2)$ effort for storage and $\mathcal{O}(P)$ for resampling. We have found this can be achieved by finding the minimal hypercube $\mathcal{H}(\mathcal{T}_E^*) \in \mathcal{P}$ which encompasses all members of the loss minimizing POPS-ensemble $\Theta_{\mathbf{X}}^* \in \mathcal{T}_E^*$. As $\mathcal{H}(\mathcal{T}_E^*)$ intersects all POPS by construction, equation (15) is satisfied by the hypercube *ansatz* uniform over $\mathcal{H}(\mathcal{T}_E^*)$, i.e.

$$\pi_{\mathcal{H}}^*(\Theta) = V_{\mathcal{H}}^{-1} \delta(\Theta \in \mathcal{H}(\mathcal{T}_E^*)), \quad (18)$$

where $V_{\mathcal{H}} = \int_{\mathcal{P}} \delta(\Theta \in \mathcal{H}(\mathcal{T}_E^*)) d\Theta$. Crucially, resampling $\pi_{\mathcal{H}}(\Theta)$ requires only $\mathcal{O}(P)$ effort whilst giving a conservative estimate and bounding of test errors.

To determine $\mathcal{H}(\mathcal{T}_E^*)$ we use singular value decomposition on the POPS-ensemble \mathcal{T}_E^* to obtain the right

eigenmatrix $\mathbf{V} \in \mathbb{R}^{R \times P}$, $R \leq P$, $\mathbf{V}\mathbf{V}^\top = \mathbb{I}_R$, requiring $\mathcal{O}(P^3)$ effort for evaluation. Uniformly sampling the full max/min hypercube of the projected ensemble $\tilde{\mathcal{T}}_E^* = \{\mathbf{V}\Theta | \Theta \in \mathcal{T}_E^*\}$ returns samples $\Theta^\top \mathbf{V}$ of $\pi_{\mathcal{H}}^*$ for $\mathcal{O}(R)$ effort and $\mathcal{O}(RP)$ storage. We find this efficient hypercube posterior to give excellent bounding and prediction of test errors for $P \in [3, 1600]$, as shown in figures 2 and 3. An additional advantage is the simplicity of implementation for linear models; an example Python code is provided in the SM [17].

POPS-constrained loss minimization for linear models

Both the ensemble and hypercube *ansatz* require POPS-constrained loss minimizing fits $\Theta_{\mathbf{X}}^* \in \mathcal{P}_{\mathcal{M}}(\mathbf{X})$. Practical application therefore requires an efficient means to perform this constrained minimization. Linear models use feature functions $\mathcal{F} : \mathcal{X} \rightarrow \mathcal{P} \times \mathcal{Y}$ to map inputs $\mathbf{X} \in \mathcal{X}$ to features $\mathbf{F}(\mathbf{X}) \in \mathcal{P} \times \mathcal{Y}$, giving $\mathcal{M}(\mathbf{X}, \Theta) = \Theta \cdot \mathbf{F}(\mathbf{X})$ with parameters $\Theta \in \mathcal{P}$. Minimizing the PAC-Bayes bound (21) with a Gaussian prior $\pi_0(\Theta) = \mathcal{N}(\Theta | \mathbf{0}, \Sigma_0)$ gives a global loss minimizer $\Theta_{\mathcal{L}}^*$ of

$$\Theta_{\mathcal{L}}^* = \mathbf{A} \langle \mathbf{F}(\mathbf{X}) \mathcal{E}(\mathbf{X}) \rangle_{\mathcal{X}}, \quad (19)$$

$$\mathbf{A} = [\Sigma_{\mathcal{Y}} \Sigma_0^{-1} / N + \langle \mathbf{F}(\mathbf{X}) [\mathbf{F}(\mathbf{X})]^\top \rangle_{\mathcal{X}}]^{-1}.$$

The epistemic covariance for small N/P can be incorporated in a variational PAC-Bayes scheme [17] that will be developed further in future work. However, in the following, we concentrate on misspecification uncertainties in the limit $N/P \rightarrow \infty$, where the influence of Σ_0 is negligible. For linear models the POPS-constraint is simply $\Theta_{\mathbf{X}} \cdot \mathbf{F}(\mathbf{X}) \equiv \mathcal{E}(\mathbf{X})$. The loss minimizing pointwise fits $\Theta_{\mathbf{X}}^*$ can be evaluated analytically via the efficient rank-one updates

$$\Theta_{\mathbf{X}}^* = \Theta_{\mathcal{L}}^* + \frac{\mathcal{E}(\mathbf{X}) - \Theta_{\mathcal{L}}^* \cdot \mathbf{F}(\mathbf{X})}{h(\mathbf{X})} \mathbf{A} \mathbf{F}(\mathbf{X}), \quad (20)$$

where $h(\mathbf{X}) = [\mathbf{F}(\mathbf{X})]^\top \mathbf{A} \mathbf{F}(\mathbf{X})$ is the *leverage*, an outlier measure closely related to the distance of [19]. The minimum loss solution is the leverage-weighted centroid of pointwise optima, $\Theta_{\mathcal{L}}^* = \langle h(\mathbf{X}) \Theta_{\mathbf{X}}^* \rangle_{\mathcal{X}}$. Equation (20) is our third main result, a scheme to incorporate misspecification uncertainty into least-squares linear regression for minimal overhead, requiring only $\mathcal{O}(N)$ inner products over feature vectors, which can then be used to construct the ensemble or hypercube *ansatz* given above. A simple python implementation is provided in the SM [17].

NUMERICAL EXPERIMENTS

Comparison to Bayesian ridge regression and minimization of \mathcal{G}_E

We applied Bayesian ridge regression and our POPS-*ansatz* to regress a quadratic polynomial against a sinusoidal function, the constant, linear and quadratic features giving $P = 3$ model parameters. The SM [17] shows the same procedure for a model with $P = 6$ independent features. For these simple models it is possible to approximately minimize the generalization error \mathcal{G}_E of some discrete model ensemble, providing we regularize with a finite aleatoric uncertainty $\Sigma_{\mathcal{Y}} = \sigma \Sigma_{\mathcal{L}}^*$. With increasing σ we have $\mathcal{G} \rightarrow \mathcal{L}$ and thus expect the ensemble to concentrate on $\Theta_{\mathcal{L}}^*$, whilst in the small σ regime of interest minimizing \mathcal{G}_E becomes increasingly unstable. We found the same small σ instability when applying an ensemble approach from [12] which targets a second-order PAC-Bayes loss bound, designed for misspecified probabilistic models where σ can be large. These instabilities show existing misspecification-aware methods require careful hyperparameter tuning and low model dimension to avoid vanishing gradients or other numerical issues. Our POPS-*ansatz*, in contrast, can easily sample $P = \mathcal{O}(1000)$ or higher dimensional data.

Figure 1 shows results for $\sigma = 1, 1/3, 1/6$, at the lower limit for which minimization converges. As expected from section , Bayesian ridge regression significantly underestimates test errors even at the 99.7% confidence level (three standard deviations) which as discussed above will worsen with increasing N/P . The max/min range of the numerical ensemble shows similar behavior for $\sigma = 1, 1/3$ whilst at $\sigma = 1/6$ test errors are bounded but significantly overestimated, which worsens as σ decreases (whilst stable). This was also seen on higher dimensional datasets [17]. Importantly, in all cases our POPS-*ansatz* π_E^* and π_H^* give excellent bounding of test errors and are stable in the near-deterministic limit $\sigma \rightarrow 0$. As expected, the hypercube *ansatz* π_H^* gave slightly more conservative bounds.

Test errors in medium-dimensional linear regression

We now consider higher/medium dimensional problems, $P = 10-50$, where numerical minimization of \mathcal{G}_E is not possible. The simulation engines were constrained to be misspecified from the linear surrogate models by combining features in quadratic, cubic or sinusoidal functions or randomly sampling the linear feature coefficients from some predetermined subset of models. A noise term that simulates the presence of variability orthogonal to the chosen feature set was also used. In all cases, independent test and training data were generated, typically with

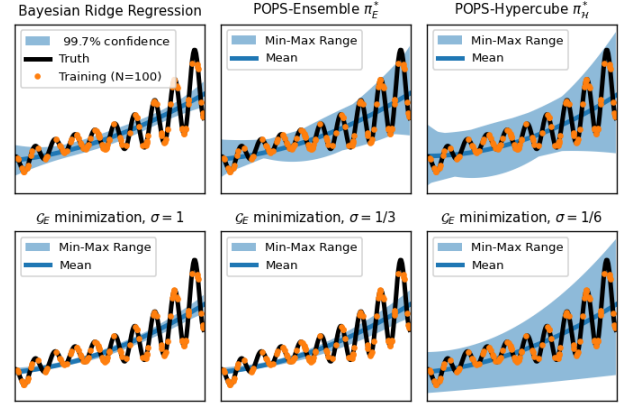


Figure 1. Regression of a deterministic quadratic polynomial ($P = 3$) model onto a sinusoidal "simulation engine", trained on $N = 100$ points. Top left: mean and 3σ interval from Bayesian ridge regression. All other plots show mean and max/min range. Top: POPS-ensemble and POPS-hypercube *ansatz* π_E^* and π_H^* . Bottom: numerically optimized \mathcal{G}_E for a uniformly weighted N -ensemble, regularized with $\Sigma_{\mathcal{Y}} = \sigma \Sigma_{\mathcal{L}}^*$, for $\sigma = 1, 1/3, 1/6$. Lower σ values gave numerical instabilities.

a 10:90 test:train split. However, all conclusions remain robust to varying the precise nature of data generation and the classes of engine considered [17].

As shown, the $\mathcal{O}(P)$ hypercube *ansatz* π_H^* provides an excellent prediction and bounding, of the test error distribution whilst the $\mathcal{O}(N)$ ensemble π_E^* underestimates moments of the error distribution and the max/min envelope bound. Importantly, the envelope violation rate of the hypercube *ansatz* π_H^* drops with N/P , as shown in figure 2 for a range of P and N/P . The simultaneous prediction and *bounding* of test errors is highly valuable for surrogate model deployment, allowing not only the prediction of expected errors but a robust assessment of worst case error scenarios. We conclude with an application of the hypercube *ansatz* to challenging high-dimensional $P = \mathcal{O}(1000)$ datasets from atomic machine learning.

High-dimensional models for atomic simulations

Atomic-scale simulations of materials were traditionally broadly classified into two types:

- Empirical simulations with physically-motivated parametric models of interatomic interactions. These allow for fast simulations at a qualitative level of accuracy.
- First-principle quantum simulations obtained from approximate solutions of the full Schrodinger equation. These incur a high computational cost and exhibit poor scalability with system size.

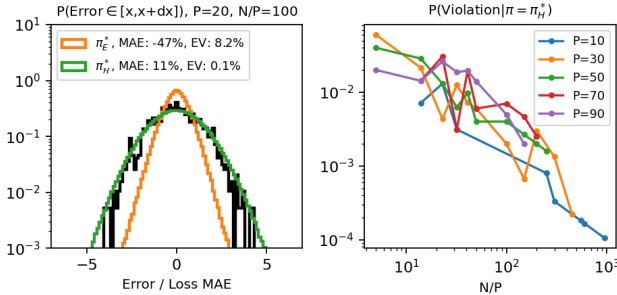


Figure 2. Test errors of a misspecified linear surrogate model on a cubic simulation engine. Left: test error histogram at $P = 20$, $N/P = 100$ for the minimum loss model (black) and predictions from the POPS-ensemble π_E^* (orange) and POPS-hypercube π_H^* (green) *ansatz*. MAE: mean absolute error relative to the minimum loss solution. EV: envelope violation, points lying outside of the max/min bound. Right: Probability of envelope violation for the π_H^* *ansatz* with P and N/P .

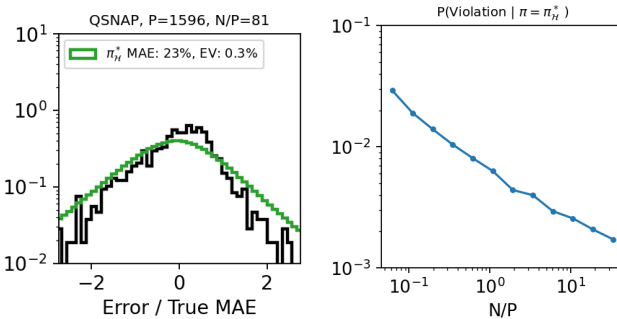


Figure 3. Application to interatomic potentials. Left: test error histogram at $P = 1596$, $N/P = 81$ for the minimum loss model (black) and predictions from the POPS-hypercube π_H^* (green) *ansatz*. MAE: mean absolute error relative to the minimum loss solution. EV: envelope violation, points lying outside of the max/min bound. Right: Probability of envelope violation for the π_H^* *ansatz* with N/P .

The advent of ML has blurred the lines between these two limits by promising near-quantum accuracy at a much more favorable computational cost and scaling [2]. The total energy of the system V is typically factored into a sum of per-atom contributions V_i , which are themselves parameterized in term of a feature vector that describes the local atomic environment $\mathbf{F}_i(\{\mathbf{x}_j | r_{ij} < r_c\})$, where r_c is a interaction range. Training an ML model then proceeds by minimizing a squared error loss between reference energies and gradients. While certain ML approaches are systematically improvable, the computational cost associated with repeated evaluations can limit the complexity of the models that are selected for applications. Further, quantum calculations can be tightly converged, so that their intrinsic error ϵ (w.r.t. a fully converged calculation) can be made small compared to

typical errors incurred by computationally-efficient models. This regime corresponds to the underparametrized deterministic setting considered here. Estimating the errors incurred by such ML models is highly sought after to assess the robustness of conclusions drawn from the simulations [20–23].

In the following, a linear surrogate model $V_i = \Theta \cdot \mathbf{F}_i$ was used to predict per-atom contributions. Numerical experiments were carried out by randomly sub-selecting N training points (either energies or gradient components), and by generating a discrete ensemble of N pointwise-optimal models according to Eq. 20, up to a maximal value of $N = 129,853$. The properties of the ensemble are then evaluated on a complementary set of 10,000 hold-out testing points. Error analysis is carried out in the context of the POPS-hypercube *ansatz*. Even on the full dataset, the analysis requires on the order of 20 minutes on 1 CPU core. It is therefore extremely lightweight in addition to being easily parallelizable, enabling its use for extremely large datasets.

The results show that the envelope violation on test data varies between 2% and 0.2% for $N/P = 0.06$ and 33, respectively, in qualitative agreement with the results shown in figure 2. This demonstrates that worst-case model errors are extremely well captured by the POPS-hypercube ensemble. As reported in the left panel of figure 3, these excellent bounds do not trivially result from the resampled error distribution being overly pessimistic, as the distribution of errors induced by a uniform parameter resampling within the POPS-hypercube provides an excellent predictor of the actual error distribution with respect to the minimum-loss model. The MAE estimated from the resampled models exceeds the measured value by only 23%, while providing a very good description of the overall error distribution.

The information generated by this simple and efficient approach will be invaluable to estimate the uncertainties on a range of different physical quantities inferred from atomistic simulations.

CONCLUSION

In spite of its ubiquity in practical applications, misspecification is often ignored in Bayesian regression approaches based on expected loss minimization, which can lead to erroneous conclusions regarding parameter uncertainty quantification, surrogate model selection, and error propagation. In this work, we show that the important near-deterministic underparameterized regime is amenable to approximation by two formally simple *ansatz* that exploits the concentration of the cross-entropy minimizing ensemble onto pointwise optimal parameter sets (POPS). For linear regression problems, this ensemble can be obtained extremely efficiently using rank-one perturbations of the expected loss solu-

tion, from which our optimally weighted POPS-ensemble or POPS-bounding hypercube *ansatz* can be efficiently obtained. Our POPS-constrained *ansatz* are shown to produce excellent parameter distributions which give accurate prediction of test error distributions and highly informative worst-case bounds on model predictions, in the important misspecified, near-deterministic regime where existing methods fail.

Synthetic test data

All synthetic data was generated with Python/JAX code, to be made available following peer review.

Atomic simulation data

Atomic training data was generated using an information-theoretic approach [5, 24]. 10,000 atomistic configurations containing between 2 and 32 tungsten atoms were generated and characterized using Density Functional Theory [25], yielding 167,922 training data points in total (10,000 energies and 157,922 gradient components). Per-atom energies are expressed as

a linear combination of $P = 1596$ so-called bispectrum components within the ‘Quadratic’ Spectral Neighborhood Analysis Potential (SNAP) formalism [26], which can be expressed as a linear surrogate model $V_i = \Theta \cdot \mathbf{F}_i(\{\mathbf{x}_j | r_{ij} < r_c\})$.

Acknowledgements

This work was initiated during a visit at the Institute for Pure and Applied Mathematics at the University of California, Los Angeles (supported by National Science Foundation (NSF) grant DMS-1925919) and continued at the Institute for Mathematical and Statistical Innovation, University of Chicago (supported by the NSF grant DMS-1929348). Their hospitality is graciously acknowledged. TDS gratefully acknowledges support from ANR grants ANR-19-CE46-0006-1 and ANR-23-CE46-0006-1, IDRIS allocation A0120913455 and an Emergence@INP grant from the CNRS. D.P. was supported by the Laboratory Directed Research and Development program of Los Alamos National Laboratory under project number 20220063DR. Los Alamos National Laboratory is operated by Triad National Security, LLC, for the National Nuclear Security Administration of U.S. Department of Energy (Contract No. 89233218CNA000001).

PAC-Bayes concentration inequalities for regression

PAC-Bayes inequalities were originally designed for classification problems where the loss function is bounded to $[0, 1]$. The extension to regression requires treatment of unbounded losses, which is discussed in detail in [16]. Determining the value of the upper bound for $C_0[\pi_0]$ in the PAC-Bayes concentration inequality (21) requires certain assumptions on the distribution of the error between the empirical and true expected loss [16]. Following [16], we assume that this error distribution is unbounded but sub-normal, i.e. all error fluctuations are bounded by a normal distribution of variance s^2 , giving $C_0[\pi_0] < s^2/2$. We refer the reader to [16] and subsequent works [12, 27] for further discussion. For completeness, we recall here the bound used in the main text:

$$\mathcal{L}[\pi] \leq \int_{\mathcal{P}} \hat{L}_N(\Theta) + \frac{1}{N} \ln \left| \frac{\pi}{\pi_0} \right| d\pi(\Theta) - \frac{\ln |\xi|}{N} + C_0, \quad (21)$$

Model selection criteria for deterministic models

The Bayesian information criterion (BIC), used to discriminate between possible surrogate models, is derived by approximating (twice) the negative log evidence as $N/P \rightarrow \infty$, assuming a slowly varying prior $\pi_0(\Theta) = \mathcal{O}(1)$. Using the above definitions we find

$$BIC = -2 \ln \left| \int \exp(-N\hat{L}(\Theta)) \pi_0(\Theta) d\Theta \right| \rightarrow N \text{Tr}(\Sigma_{\mathcal{L}}^* \Sigma_{\mathcal{Y}}^{-1}) + \ln (\|\Sigma_{\mathcal{Y}}\|^N N^P \|\mathcal{I}_{\mathcal{L}}^*\|) + \mathcal{O}(1). \quad (22)$$

We note that the value of the PAC-Bayes loss bound (21) satisfies $BIC = 2N\hat{L}_N[\pi_{\mathcal{L},N}] - 2C_0$, with C_0 model independent, as discussed in [16]. In standard derivations $\Sigma_{\mathcal{Y}}$ is set to the variational maximum likelihood solution $\Sigma_{\mathcal{Y}} = \Sigma_{\mathcal{L}}^*$, yielding the familiar expression $BIC = P \ln N + N \ln \|\Sigma_{\mathcal{L}}^*\| + \ln \|\mathcal{I}_{\mathcal{L}}^*\|$, where model independent terms are neglected. However, for deterministic regression problems, $\Sigma_{\mathcal{Y}}$ is fixed. Neglecting model-independent terms, this gives an alternative BIC for deterministic models of

$$BIC = N \text{Tr}(\Sigma_{\mathcal{L}}^* \Sigma_{\mathcal{Y}}^{-1}) + P \ln N + \ln \|\mathcal{I}_{\mathcal{L}}^*\|. \quad (23)$$

Summary of Laplace's method

Laplace's method, also known as the steepest descents method, is a well-known identity allowing the evaluation of an integral of an exponentiated function multiplied by a large number. The method applies to a function $f(x)$ which is twice differentiable and has a unique maximum in some closed interval $[a, b]$ which may be the entire real line. This encompasses all applications in this paper; the extension to multidimensional functions is straightforward. Laplace's method then reads

$$\lim_{N \rightarrow \infty} \int_a^b \exp[Nf(x)]dx = \sqrt{\frac{2\pi}{N}} \sqrt{\frac{d^2f((x))}{dx^2}}^{-1} \exp[N \max_{x \in [a,b]} f(x)]. \quad (24)$$

POPS-constrained ensemble *ansatz*

Selecting some set of pointwise fits and $\mathcal{T}_E = \{\Theta_{\mathbf{X}} \in \mathcal{P}_{\mathcal{M}}(\mathbf{X})\}_{\mathcal{X}}$ and weights $\mathcal{W}_E = \{w_E(\mathbf{X}) > 0\}_{\mathcal{X}}$ such that $\langle w_E(\mathbf{X}) \rangle_{\mathcal{X}} = 1$, the covering constraint is satisfied by

$$\pi_E(\Theta | \mathcal{T}_E, \mathcal{W}_E) \equiv \langle w_E(\mathbf{X}) \mathcal{N}(\Theta | \Theta_{\mathbf{X}}, [\Sigma_0 + N\mathcal{I}_{\mathcal{L}}^*]^{-1}) \rangle_{\mathcal{X}}, \quad (25)$$

For any choice of weights \mathcal{W}_E , an approximate optimal set $\Theta_{\mathbf{X}}^* \in \mathcal{T}_E^*$ can be determined in a variational setting at finite N , using (25) in the PAC-Bayes loss bound (21) for the loss $\mathcal{L}[\pi_E] = \langle w_E(\mathbf{X}) L(\Theta_{\mathbf{X}}) \rangle_{\mathcal{X}}$. As $P/N \rightarrow 0$ we show in the sub-section below this reduces to the set of POPS-constrained loss minimizers

$$\Theta_{\mathbf{X}}^* \in \mathcal{T}_E^*, \quad \Theta_{\mathbf{X}}^* \equiv \arg \min_{\Theta_{\mathbf{X}} \in \mathcal{P}_{\mathcal{M}}(\mathbf{X})} L(\Theta_{\mathbf{X}}) \quad (26)$$

The POPS-constrained loss-minimization ensures the fits will be as close as possible under the Fisher metric $\mathcal{I}_{\mathcal{L}}^*$, such that $\Theta_{\mathbf{X}}^* \rightarrow \Theta_{\mathcal{L}}^*$ for specified models. Under misspecification, the generalization error of (25) using \mathcal{T}_E^* has the $P/N \rightarrow 0$ limit

$$\mathcal{G}_0[\pi_E] = - \langle \ln \langle w_E(\mathbf{X}') m_{\mathcal{E}}(\Theta_{\mathbf{X}}^*, \mathbf{X}) \rangle_{\mathbf{X}' \in \mathcal{X}} \rangle_{\mathbf{X} \in \mathcal{X}}. \quad (27)$$

In general we expect a uniform weighting $w_E(\mathbf{X}) = 1$ to be sub-optimal for generalization as the loss-minimizing fits $\Theta_{\mathbf{X}}^*$ will be too close to $\Theta_{\mathcal{L}}^*$.

To optimize $w_E(\mathbf{X})$ we define a density $\rho_{\mathbf{X}}^*(\mathbf{X}') = m_{\mathcal{E}}(\Theta_{\mathbf{X}}^*, \mathbf{X}) / \langle m_{\mathcal{E}}(\Theta_{\mathbf{X}}^*, \mathbf{X}) \rangle_{\mathbf{X}' \in \mathcal{X}}$ of pointwise fits $\Theta_{\mathbf{X}}^*$, satisfying $|\mathcal{M}(\mathbf{X}, \Theta_{\mathbf{X}}^*) - \mathcal{E}(\mathbf{X})| = \mathcal{O}(\epsilon)$, then use Jensen's inequality to write the "loss-like" bound

$$\begin{aligned} \mathcal{G}_0[\pi_E] &= \mathcal{G}_U - \langle \ln \langle w_E(\mathbf{X}') \rho_{\mathbf{X}}^*(\mathbf{X}') \rangle_{\mathbf{X}' \in \mathcal{X}} \rangle_{\mathbf{X} \in \mathcal{X}} \\ &\leq \mathcal{G}_U - \langle \ln |w_E(\mathbf{X}')| \langle \rho_{\mathbf{X}}^*(\mathbf{X}') \rangle_{\mathbf{X} \in \mathcal{X}} \rangle_{\mathbf{X}' \in \mathcal{X}}, \end{aligned} \quad (28)$$

where \mathcal{G}_U is the generalization error (27) with uniform weighting $w_E(\mathbf{X}) = 1$. Under the constraint $\langle w_E(\mathbf{X}) \rangle_{\mathcal{X}} = 1$ it is simple to show this upper bound is minimized by

$$w_E^*(\mathbf{X}) \in \mathcal{W}_E^*, \quad w_E^*(\mathbf{X}) = \lambda \langle \rho_{\mathbf{X}}^*(\mathbf{X}) \rangle_{\mathbf{X}' \in \mathcal{X}}. \quad (29)$$

where λ ensures $\langle w_E^*(\mathbf{X}) \rangle_{\mathcal{X}} = 1$. Evaluation requires at most $\mathcal{O}(N^2)$ effort but only $\mathcal{O}(N)$ for storage and resampling. The final ensemble *ansatz* parameter posterior then reads

$$\pi_E^*(\Theta) \equiv \langle w_E^*(\mathbf{X}) \delta(\Theta - \Theta_{\mathbf{X}}^*) \rangle_{\mathcal{X}}. \quad (30)$$

Equation (30) is a variationally optimized ensemble *ansatz* for misspecified regression problems. The worst case of extreme misspecification, corresponding to non-intersecting POPS $\mathcal{P}_{\mathcal{M}}(\mathbf{X}') \cap \mathcal{P}_{\mathcal{M}}(\mathbf{X}) = \emptyset$, gives $\rho_{\mathbf{X}'}^*(\mathbf{X}) = \delta_{\mathbf{X}\mathbf{X}'}$ and thus uniform weights $w_E^*(\mathbf{X}) = 1$. Interestingly, it is simple to see we have uniform weighting at large ϵ as $\rho_{\mathbf{X}}^*(\mathbf{X})$ is uniform. For real systems we find $w_E^*(\mathbf{X})$ is highly non-uniform and smallest for points near to $\Theta_{\mathcal{L}}^*$, as expected. However, numerical test reveal moments of the predicted ensemble errors are still underestimated, as the "loss like" bounds still bring all points too close to the minimum loss value, which motivates the hypercube approach described in the text. However, the max/min bounds of the ensemble, which are insensitive to our choice of $w(\mathbf{X})$, remain robust, as shown in figure 1.

Variational optimization

For finite N/P , we have access to training data $\mathcal{D}_N = \{\mathbf{Y}_i, \mathbf{X}_i\}_{i=1}^N$ to give averages over $\langle \dots \rangle_N$, with some set of pointwise fits $\mathcal{T}_E = \{\Theta_i\}_{i=1}^N$, $\Theta_i \in \mathcal{P}_M(\mathbf{X}_i)$. Our ensemble *ansatz* then reads

$$\pi_E(\Theta) = \langle w_{E,i} \mathcal{N}(\Theta | \Theta_i, \sigma^2 \mathbb{I}) \rangle_N = \sum_{\mathbf{X}_i \in \mathcal{D}_N} w_{E,i} w_i \mathcal{N}(\Theta | \Theta_i, \sigma^2 \mathbb{I}), \quad (31)$$

where $w_{E,i}$ are the discrete ensemble weights and w_i are the training data weights.

The empirical loss $\hat{\mathcal{L}}_N[\pi_E]$, which contributes All π -dependent terms in the PAC-Bayes upper bound (21) then read

$$\hat{\mathcal{L}}_N[\pi_E] = \int \hat{L}_N(\Theta) \pi_E(\Theta), \quad KL(\pi_E | \pi_0) = \int \ln \left| \frac{\pi_E(\Theta)}{\pi_0(\Theta)} \right| \pi_E(\Theta) d\Theta. \quad (32)$$

To proceed, we define a POPS-constrained variation $\delta_i \Theta_i$ such that $\Theta_i + \delta_i \Theta_i \in \mathcal{P}_M(\mathbf{X}_i)$, which gives a variation in π_E of

$$\delta_i \pi_E(\Theta) \equiv \frac{w_{E,i} w_i}{\sigma^2} \delta \Theta_i^\top [\Theta - \Theta_i] \mathcal{N}(\Theta | \Theta_i, \sigma^2 \mathbb{I}). \quad (33)$$

The upper bound (21) thus has a POPS-constrained variation

$$\begin{aligned} \delta_i \left(\hat{\mathcal{L}}_N[\pi_E] + \frac{1}{N} KL(\pi_E | \pi_0) \right) &= \frac{w_{E,i} w_i}{\sigma^2} \int \delta \Theta_i^\top [\Theta - \Theta_i] \left(\hat{L}_N(\Theta) + \frac{1}{N} \ln \left| \frac{\pi_E(\Theta)}{\pi_0(\Theta)} \right| \right) \mathcal{N}(\Theta | \Theta_i, \sigma^2 \mathbb{I}) d\Theta, \\ &= w_{E,i} w_i \delta_i \Theta_i^\top \int \nabla_\Theta \left(\hat{L}_N(\Theta) + \frac{1}{N} \ln \left| \frac{\pi_E(\Theta)}{\pi_0(\Theta)} \right| \right) \mathcal{N}(\Theta | \Theta_i, \sigma^2 \mathbb{I}) d\Theta, \end{aligned} \quad (34)$$

where we use integration by parts. Aside from the POPS constrained variation, this is a standard variational result which in principle allows for variational minimization of $\pi_E(\Theta)$ at finite N for both linear and non-linear models. An alternative POPS-constrained variational approach for linear regression at finite N is provided in appendix ??.

In the limit $\sigma \rightarrow 0$ we make the approximation that, for $\Theta - \Theta_i = \delta \Theta$, $\pi_E(\Theta_i + \delta \Theta) \simeq (1/N) \mathcal{N}(\delta \Theta | \mathbf{0}, \sigma^2 \mathbb{I})$. With a Gaussian prior of zero mean and covariance Σ_0 we have

$$\int \nabla_\Theta \ln \left| \frac{\pi_E(\Theta)}{\pi_0(\Theta)} \right| \mathcal{N}(\Theta | \Theta_i, \sigma^2 \mathbb{I}) d\Theta = \int \left(\frac{\Theta - \Theta_i}{\sigma^2} + \Sigma_0^{-1} \Theta \right) \mathcal{N}(\Theta | \Theta_i, \sigma^2 \mathbb{I}) d\Theta \rightarrow \Sigma_0^{-1} \Theta_i, \quad \sigma \rightarrow 0. \quad (35)$$

In the present work we are primarily concerned with the underparametrized, or large data limit $P/N \rightarrow 0$, where the influence of the prior distribution is negligible, as demonstrated in the main text. In this regime, for small σ the variation of the upper bound (21) has a limiting form of

$$\delta_i \hat{\mathcal{L}}_N[\pi_E] = w_{E,i} w_i \delta_i \Theta_i^\top \left[\nabla_\Theta \hat{L}_N(\Theta_i) + \frac{1}{N} \Sigma_0^{-1} \Theta_i \right] + \mathcal{O}(\sigma^2). \quad (36)$$

This result shows the POPS-constrained variation of the PAC-Bayes loss upper bound converges to the gradient of the squared loss evaluated at a POPS-constrained parameter choice, to within a positive multiplicative constant. As a result, in the underparametrized limit the variational optimal choice of of POPS-constrained parameter Θ_X will be given by

$$\Theta_i^* \equiv \arg \min_{\Theta \in \mathcal{P}_M(\mathbf{X}_i)} L(\Theta), \quad (37)$$

in agreement with the result given in the main text.

Implementation of the *ansatz* in Python

The hypercube projector $\mathbf{V} \in \mathbb{R}^{R \times P}$ and bounds $\mathbf{B} \in \mathbb{R}^{R \times 2}$ can be produced with the following python code, where \mathbf{A}^T is the transpose of \mathbf{A} :

```

1 import numpy as np
2 def hypercube(X,y,prior,thresh=1e-8):
3     # X.shape = (N,P), y.shape = (N,)
4     # Inverse of A with prior matrix
5     A_i = np.dot(X.T,X) + prior / y.size
6     # Minimum loss solution
7     T_L = np.linalg.solve(A_i,np.dot(X.T,y))
8     # Minimum loss errors
9     e = y - np.dot(X, T_L)
10    # Leverage of each point
11    X_dot_A = np.linalg.solve(A_i,X.T)
12    h = (X * X_dot_A).sum(1)
13    # Pointwise fits, shape = (P,N)
14    T = np.multiply(X_dot_A, e/h)
15    # Find hypercube projector
16    nu,V = np.linalg.eigh(T@T.T)
17    nu_sel = nu<nu.max()*thresh
18    V = V[nu_sel,:]
19    # bounds
20    B = np.array([(T@V.T).max(0),(T@V.T).min(0)]).T
21    return V,B

```

To sample the ensemble we use uniform random numbers

```

1 import numpy as np
2 def resample(V,B,n=20,seed=123):
3     np.random.seed(seed)
4     u = np.random.uniform(
5         min=B[:,0],
6         max=B[:,1],
7         size=(n,V.shape[0]))
8     return u@V

```

Additional plots of test error prediction

Low dimensional models

We applied the same procedure as for the polynomial example to a model system with $P = 6$ independent features to simulate more realistic datasets. As before, the numerical minimization routine could only treat a small range of σ values. Figure 4 shows the resulting parameter distributions. At large $\sigma = 2$ the minimizer quickly concentrates all ensemble members on the minimum loss solution; at $\sigma = 1$ the ensemble distribution is notably sharper than the POPS-ensemble π_E^* , whilst for low sigma $\sigma = 1/2$ the minimization only has marginal stability, but becomes closer to the POPS-bounding hypercube $\pi_{\mathcal{H}}^*$. In addition, a minimizer initialized with the POPS-ensemble did not change appreciably. These albeit simple results give strong evidence that our *ansatz* is indeed a stable and highly efficient means to find approximate minimizers of \mathcal{G} that would otherwise be intractable.

Medium dimensional models

The plots below are identical in presentation to the top row of figures in the main text, but for the quadratic and random linear simulation engines described in the main text.

* thomas.swinburne@cnrs.fr

† danny.perez@lanl.gov

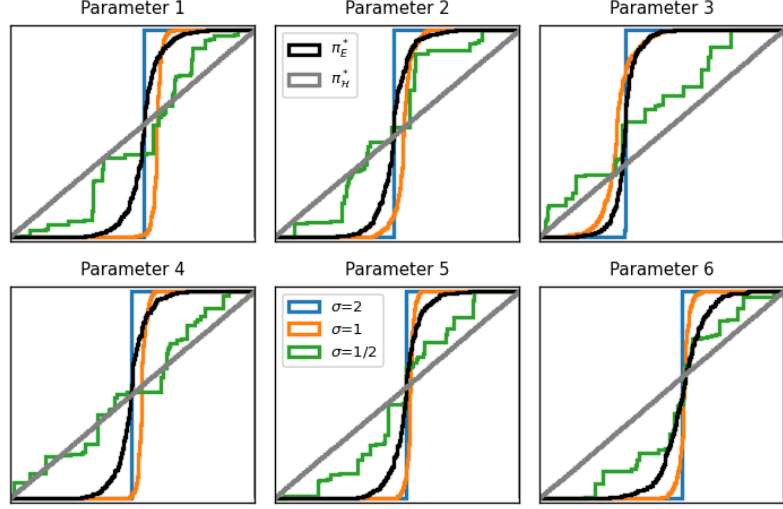


Figure 4. Regression of a linear model onto a cubic "simulation engine" with $P = 6$ independent features, trained on $N = 500$ points. The panels show the cumulative distribution of each parameter across the N -member ensemble. Black, gray : ensemble and hypercube ansatz π_E^* and π_H^* . Blue, orange and green : numerically optimized \mathcal{G}_E for a uniformly weighted N -ensemble, regularized with $\Sigma_{\mathcal{Y}} = \sigma \Sigma_{\mathcal{L}}^*$, for $\sigma = 2, 1, 1/2$. As in Figure 1 in the main text, lower σ gave numerical instabilities.

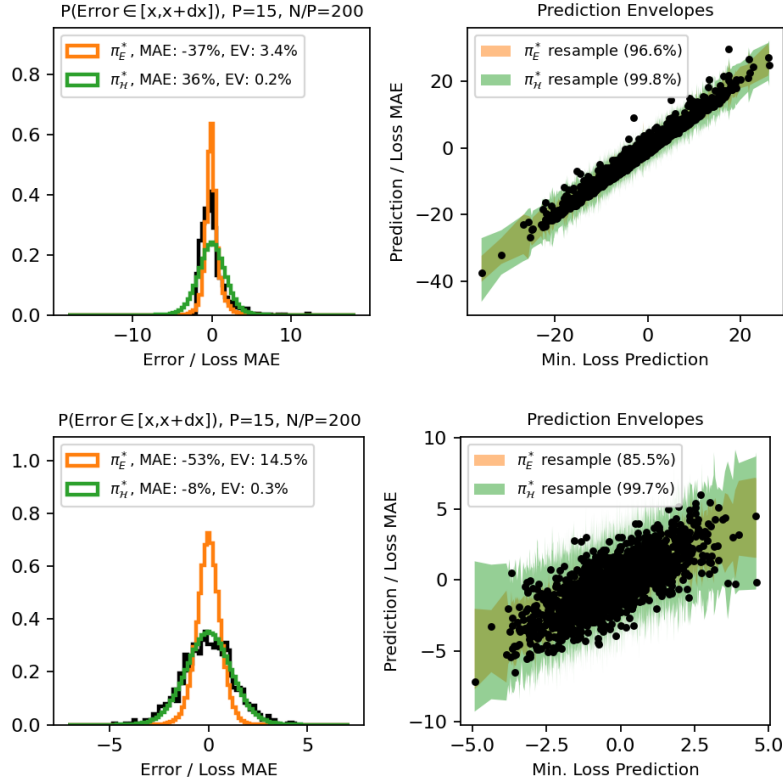


Figure 5. Test error prediction for medium dimensional problems. Left: Observed test errors for a misspecified linear surrogate model ($P=15$) on a quadratic (top) and random linear (bottom) simulation engine, along with predicted test errors from the POPS-ensemble. Right: Parity plots for the minimum loss model, along with envelope bounds from the POPS-ensemble and hypercube.

- [2] V. L. Deringer, M. A. Caro, and G. Csányi, *Advanced Materials* **31**, 1902765 (2019).
- [3] C. Lapointe, T. D. Swinburne, L. Thiry, S. Mallat, L. Proville, C. S. Becquart, and M.-C. Marinica, *Physical Review Materials* **4**, 063802 (2020).
- [4] C. Nyshadham, M. Rupp, B. Bekker, A. V. Shapeev, T. Mueller, C. W. Rosenbrock, G. Csányi, D. W. Wingate, and G. L. Hart, *npj Computational Materials* **5**, 51 (2019).
- [5] D. Montes de Oca Zapiain, M. A. Wood, N. Lubbers, C. Z. Pereyra, A. P. Thompson, and D. Perez, *npj Computational Materials* **8**, 189 (2022).
- [6] C. Bonatti, B. Berisha, and D. Mohr, *International Journal of Plasticity* **158**, 103430 (2022).
- [7] J. Kudela and R. Matousek, *Soft Computing* **26**, 13709 (2022).
- [8] S. Lahlou, M. Jain, H. Nekoei, V. I. Butoi, P. Bertin, J. Rector-Brooks, M. Korablyov, and Y. Bengio, arXiv preprint arXiv:2102.08501 (2021).
- [9] A. F. Psaros, X. Meng, Z. Zou, L. Guo, and G. E. Karniadakis, *Journal of Computational Physics* **477**, 111902 (2023).
- [10] P. Alquier, arXiv preprint arXiv:2110.11216 (2021).
- [11] W. R. Morningstar, A. Alemi, and J. V. Dillon, in *International Conference on Artificial Intelligence and Statistics* (PMLR, 2022) pp. 8270–8298.
- [12] A. Masegosa, *Advances in Neural Information Processing Systems* **33**, 5479 (2020).
- [13] Y. Kato, D. M. Tax, and M. Loog, arXiv preprint arXiv:2210.16938 (2022).
- [14] S. Lotfi, P. Izmailov, G. Benton, M. Goldblum, and A. G. Wilson, in *International Conference on Machine Learning* (PMLR, 2022) pp. 14223–14247.
- [15] G. Imbalzano, Y. Zhuang, V. Kapil, K. Rossi, E. A. Engel, F. Grasselli, and M. Ceriotti, *The Journal of Chemical Physics* **154** (2021).
- [16] P. Germain, F. Bach, A. Lacoste, and S. Lacoste-Julien, *Advances in Neural Information Processing Systems* **29** (2016).
- [17] T. Swinburne and D. Perez, “Supplementary material,” (2024).
- [18] W. Hoeffding, *The collected works of Wassily Hoeffding*, 409 (1994).
- [19] P. C. Mahalanobis, in *Proceedings of the National Institute of Science of India* (National Institute of Science of India, 1936).
- [20] M. Wen and E. B. Tadmor, *npj computational materials* **6**, 124 (2020).
- [21] Y. Li, W. Xiao, and P. Wang, in *ASME International Mechanical Engineering Congress and Exposition*, Vol. 52170 (American Society of Mechanical Engineers, 2018) p. V012T11A030.
- [22] J. J. Gabriel, N. H. Paulson, T. C. Duong, F. Tavazza, C. A. Becker, S. Chaudhuri, and M. Stan, *JOM* **73**, 149 (2021).
- [23] S. Wan, R. C. Sinclair, and P. V. Coveney, *Philosophical Transactions of the Royal Society A* **379**, 20200082 (2021).
- [24] M. Karabin and D. Perez, *The Journal of Chemical Physics* **153** (2020).
- [25] W. Kohn and L. J. Sham, *Phys. Rev.* **140**, A1133 (1965).
- [26] M. A. Wood and A. P. Thompson, *The Journal of chemical physics* **148** (2018).
- [27] V. Shalaeva, A. F. Esfahani, P. Germain, and M. Petreczky, in *Proceedings of the AAAI Conference on Artificial Intelligence*, Vol. 34 (2020) pp. 5660–5667.